Optical Materials 92 (2019) 319–329

Contents lists available at ScienceDirect

Optical Materials

journal homepage: www.elsevier.com/locate/optmat

# Evaluation of CdS/CdTe thin film solar cells: SCAPS thickness simulation and analysis of optical properties

L.I. Nykyruy[a], R.S. Yavorskyi[a,*], Z.R. Zapukhlyak[a], G. Wisz[b], P. Potera[b]

[a] Vasyl Stefanyk Precarpathian National University, T. Shevchenko, 57, 76-018, Ukraine
[b] Department of Experimental Physics, Faculty of Mathematics and Natural Sciences, University of Rzeszow, Pigonia 1 Street, Rzeszow, 35-317, Poland

ARTICLE INFO

*Keywords:*
Thin films
Solar cells simulation
Cadmium telluride
Heterojunction
Thermal evaporation method
Optical properties

ABSTRACT

The paper presents the study of the optical properties of a thin layer of Cadmium Sulphide deposited on Cadmium Telluride films. CdTe thin films were obtained by vapor phase condensation method with different thicknesses on glass substrates. The optical properties of the deposited films were analyzed by Swanepoel method using transmission spectra. The upper thin layer of CdS was deposited by thermal evaporation method on CdTe thin films. The change of the optical properties of CdS/CdTe heterojunctions were investigated and compared with CdTe thin films. The main optical constants, such as refractive index and absorption coefficient were calculated. Advanced simulations were performed in SCAPS for optimization of CdS/CdTe thin film heterostructures.

## 1. Introduction

Thin film PV solar cell has been considered as one of the most promising solar cells due to its high-energy conversion efficiency, low cost and convenience for large-scale production. The most successful thin film solar cells are cadmium telluride (CdTe), copper indium gallium selenide (CIGS) and amorphous silicon (a-Si) with efficiencies of 18.3%, 20% and 12.3%, respectively [1]. It was reported that CdTe technology is about 30% cheaper than CIGS technology and about 40% cheaper than a-Si technology [2]. Hence, the using of CdTe-based thin film solar cells the highest ratio “efficiency/cost” can be achieved.

Materials for thin film solar cells are currently the subject of multiple researches. First Solar Corporation (the largest CdTe-based solar cells manufacturer) reported fleet average efficiencies increasing from 12.9% in 2012 to 16.6% in 2016 for their CdTe modules (First Solar, 2017). Nowadays for CdTe cells module the highest value of efficiency is 18.6%. The best value of efficiency for CIGS modules is 17.5% (Green et al., 2018). There is also a significant industrial production based on CdTe/CdS solutions, represented to a large extent by American corporation First Solar, which is a supplier of PV modules used in the currently largest Agua Caliente Solar Project solar power plant in Arizona [3]. It should be noted that thin film technology based on CdTe is the first technology that has allowed to reduce the production costs of solar energy to 0.57 $/Wp [4].

CdS forms a good heterostructure in combination with CdTe. It is a very promising material for thin film photovoltaics and offers a number of interesting advantages compared to the bulk silicon devices [5]. Because of appropriate band gap and high absorption coefficient for solar radiation the real efficiency of PV solar cells based on the n-CdS/p-CdTe heterojunction in a superstrate structure currently is 20.4% [6]. The theoretical efficiency of CdS/CdTe solar cells is predicted to be up to 28–30% [7,8]. In spite of the 10% displacement in the lattice constants of CdS and CdTe, they form an electrically excellent heterojunction, as shown by its high fill factors up to FF = 0.75 in the produced devices.

CdTe serves as the main candidate for thin-film solar cells. It is a direct band gap material with a large absorption coefficient. CdTe is a stable compound that can be obtained by wide variety of methods. CdTe thin film is sufficient to produce highly efficient cells if both bulk and surface recombination are suppressed. Rapid interest in the PV industry based on CdTe has led to different manufacturing methods.

The first significant CdTe cell in laboratory conditions was reported in 1972 by Bonnet and Rabnehorst (Fig. 1) who developed a thin film CdTe—CdS p-n heterojunction solar cell with 6% efficiency. This cell was created in a three-step process involving vapor growth of CdTe and vacuum deposition of CdS [9].

Further explore of heterojunction solar cell based on CdS/CdTe was conducted by Bube and others [10], received efficiency value is 8.4%. CdS/CdTe solar cells have a visible cost advantage in comparison to single-crystal silicon solar cells. Efforts to establish fabrication

* Corresponding author.
*E-mail address:* roctyslaw@gmail.com (R.S. Yavorskyi).

https://doi.org/10.1016/j.optmat.2019.04.029
Received 13 December 2018; Received in revised form 26 March 2019; Accepted 14 April 2019

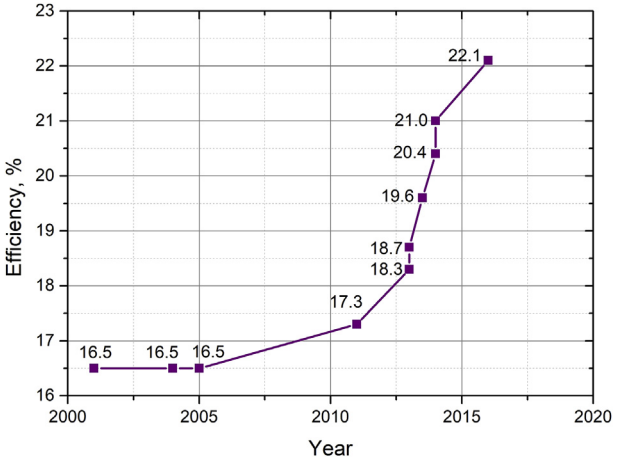


**Fig. 1.** Best laboratory efficiency of CdTe solar cells.

techniques for solar cells with improved conversion efficiencies are shown through the inventions of Eastman Kodak Company [11] where polycrystalline CdS/CdTe heterojunction cell resulted in a conversion efficiency of 8.9%.

Wu et al. at NREL [12] took a particular approach by modifying the conventional $SnO_2$/CdS/CdTe device structure and shifted a focus in research to the improvement of the TCO layer. CdTe cells operate best in a superstrate configuration, where light enters the active junction through the glass, the transparent front contact is deposited first and must survive all subsequent deposition steps. In order to improve the FF and the efficiency, Wu et al. [13] developed an oxygenated nano-rystalline CdS:O window layer with a higher optical bandgap than the poly-CdS film. The authors continued their work [13] and reported efficiencies of 16.5%.

The same efficiency of 16.5% was additionally achieved by Acevedo in 2005 [14]. Their results let to the speculation that there is a presence of a CdSTe alloy film due to the diffusion.

After 2011, the rapid development of photovoltaic solar cells based on the CdS/CdTe heterojunctions began to increase as well as the values of their efficiency. First Solar Company has dominated the past decade and continues to create solar cells that demonstrate the highest efficiency values: 18.7%, 19.6%, 20.4%, and 21% [15–21].

CdTe are relatively new technologies, and are more promising in terms of energy conversion efficiency [22].

Nowadays a lot of methods have been developed for the production of CdTe thin films. In this paper, the thin film heterojunctions were obtained using physical vapor deposition technique by thermal evaporation method [23]. This method does not require high production cost and makes the cost of thin film solar cell technology more competitive.

The transmittance properties of CdS deposited film are critical factors for the n-type window layer of CdTe-based solar cell because the light should penetrate CdS layer first before reaching the CdTe absorber layer [24]. In order to calculate the refractive index from optical transmittance spectra the extremes of the interference fringes of transmission spectrum should be used only [25,26]. The method proposed by Swanepoel [27] used to derive the real and imaginary parts of the complex refractive index and the thickness of semiconductor film. Using materials with comparatively higher optical absorption coefficient makes possible to reduce both the thickness of active photovoltaic cell layers [28], and the possible weight of photovoltaic devices depending on the used substrate.

There are number of papers theoretically focused on investigation of the efficiency dependence of CdS/CdTe thin film heterojunction on some properties [29–33]. Therefore, this study has a great importance in the field of interest of several international research centers for further industry development of highly efficient devices and manufacture of the solar cells based on heterojunctions.

**Table 1**
Technological parameters of CdTe and CdS/CdTe thin films.

| Sample number | Substrate temperature $T_S$, K | Evaporation temperature $T_E$, K | Deposition time τ, sec | Thickness d, nm |
|---|---|---|---|---|
| CdTe/glass | | | | |
| 21 | 470 | 845 | 180 | 1485 |
| 24 | 470 | 845 | 160 | 1215 |
| CdS/CdTe/glass | | | | Total thickness |
| 21 | 470 | 1150 | 45 | 1689 |
| 24 | 470 | 1150 | 30 | 1490 |

## 2. Experimental

On the first step, the CdTe thin films have been deposited on the cleaned glass substrates by thermal evaporation method. In the used installation series (5–15 films) in single cycle for various technological parameters: different thickness $d$ = (0,01–12) μm at constant deposition temperature $T_S$ = (300–570) K; uniform thickness d with different $T_S$; different evaporation temperature $T_E$ (600–1370) K at a constant thickness d or deposition temperature $T_S$ can be obtained. The thermal evaporation method is advantageous among other modern technologies (namely, molecular beam epitaxy, metal organic chemical vapor deposition, pulsed laser deposition, close spaced sublimation or RF magnetron sputtering methods) because of low prices of final products.

For researching CdTe thin films with different thicknesses (different deposition time $\tau$) at constant $T_S$ and $T_E$ (Table 1) were obtained. The growth temperature $T_s$ was 470 K, the evaporation temperature of presynthesized CdTe compounds was $T_E$ = 870 K for CdTe layer and $T_E$ = 1150 K for CdS layer. The thicknesses of thin films was set by deposition time τ = (30–180) sec. The next layer of CdS was deposited on CdTe thin film by thermal evaporation method. The technological parameters are shown in Table 1.

The samples thickness was analyzed using Bruker Dektak XT profilometer. Optical transmission spectra investigated by measuring transmittance T at normal incidence and room temperature. The measurements were carried out in the wavelength range of (180–3300) nm with 1 nm step using Agilent Technologies Cary Series UV–Vis–NIR Spectrophotometer.

For analysis of transmission spectrum the Swanepoel method was used for calculating the optical constants of the film, such as refractive index $n$, film thickness $d$ and absorption coefficient $\alpha$.

Advanced simulations were performed in the electrical solar cell simulation SCAPS software (Solar Cell Capacitance Simulator) for optimization thickness of CdS/CdTe thin film heterojunction.

## 3. Results and discussion

### 3.1. Numerical simulations

At present, interests in numerical simulation have a great importance for understanding physical properties and design of solar cells based on crystalline, polycrystalline and amorphous materials [34–38]. Numerical simulation is necessary to interpret the advanced measurements on complex structures, design and optimization of advanced cell structures.

It is difficult to analyze measurements without the precise model. Therefore, SCAPS simulator is used in this research to analyze numerically the performances of the proposed CdS/CdTe thin film heterostructure. SCAPS is a graphic solar cell simulation program, developed with LabWindows/CVI of National Instruments, at the department

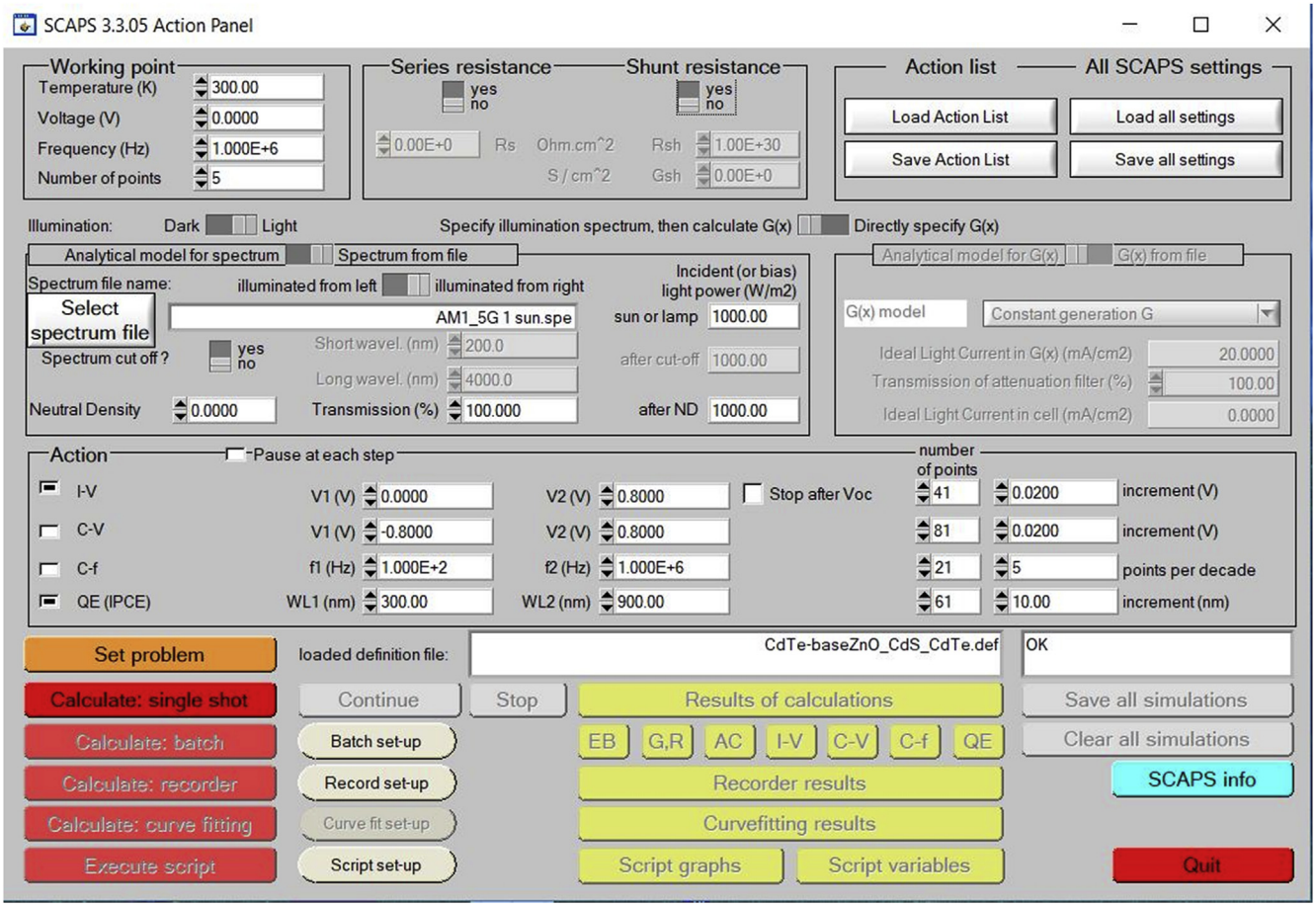


**Fig. 2.** The SCAPS start-up panel.

of Electronics and Information Systems (ELIS) of the University of Gent in Belgium by Professor Marc Burgelman [39]. A description of the program and the algorithms that it uses can be found in references [40–44].

SCAPS was used for simulating of the J-V characteristics of CdS/CdTe solar cell. The main screen which pops up after running the SCAPS is shown in Fig. 2. Dashboard contains a series of operations.

The user can get results in the form of following characteristics: I–V, C–V, C-f, Q(λ), electric field, band diagrams, carrier densities, partial recombination currents. In SCAPS software the parameters of materials and an operating point can be set: the temperature, the voltage, the frequency and illumination. Simple models have been used to obtain the temperature dependence of the effective density of states and of the thermal velocity. Other parameters such as the band gap and the mobilities are temperature independent. The task is solved by click on the bottom SET PROBLEM in the startup panel. Fig. 3 shows the SCAPS solar cell definition panel.

Specific parameters for each layer can be set. The material properties of the layers and contacts were selected from Refs. [44–48] and set by technological regimes of this research. Table 2 shows the parameters used in SCAPS simulations.

For interface recombination, SCAPS uses Pauwells Vanhoutte's model [39]. The model considers four bands for interface states i.e. conduction and valence bands of both semiconductors at the interface. This model examines the electron-hole recombination between two semiconductors (the recombination of electrons of one semiconductor with holes of another semiconductor) with standard recombination of electrons with holes within the same semiconductor. In this case, the recombination of the window layer of electrons with the absorber holes layer is the most important recombination path. The total charge in the interface states equals the discontinuity in the dielectric displacement at the interface. During the simulation process, the energy band gap diagram of n–CdS/p–CdTe heterojunction is shown in Fig. 4.

The fill factor (FF), the open-circuit voltage $V_{oc}$, the current density $J_{sc}$ and the photoenergy conversion efficiency η were acquired as photovoltaic parameters [49]. In particular, the FF was obtained by the following equation:

$$FF = \frac{I_{max} \cdot V_{max}}{I_{sc} \cdot V_{oc}} \quad (1)$$

where $I_{max}$ and $V_{max}$ are the photocurrent and the photovoltage for maximum power output, respectively, and $I_{SC}$ is the short-circuit photocurrent. Finally, the η parameter has been determined by relation:

$$\eta = \frac{I_{sc} \cdot V_{oc} \cdot FF}{P_{in}} \quad (2)$$

CdTe is an active part of the solar cell, where the largest generation and accumulation of carriers occurs (see Fig. 5). In simulation, the thickness of this layer initially varied from 0.5 μm to 5 μm with 0.5 μm step and then was set at 3 μm, while other parameters remained constant. It has been determined that at the thickness of cadmium telluride absorbing layer d = 3 μm, the efficiency η reaches the maximum value of 12.18% (Fig. 6), while the fill factor FF increases with a decrease in thickness, and in this study it takes 70.74% at the thickness d = 0.5 μm of CdTe layer.

The optimization of CdS/CdTe heterojunction solar cell has been simulated based on the above listed properties of the absorbing and window layers in Table 2. To compare, we can note that the standard material parameters were used from the SCAPS file "CdTe-base.def" in Ref. [40] and it was observed that the fill factor was 62.7%, the

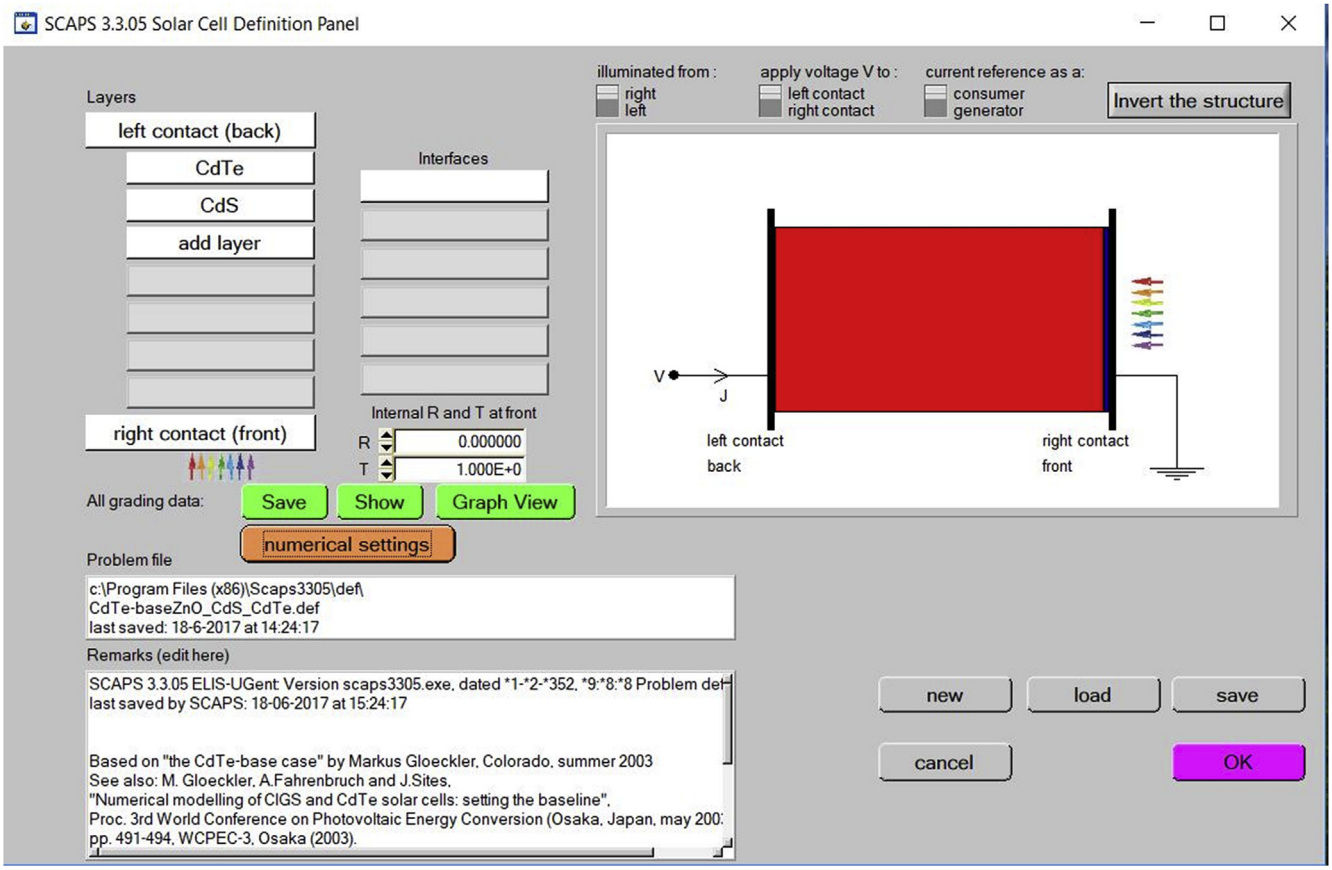


**Fig. 3.** The SCAPS solar cell definition panel.

**Table 2**
Material parameters used for simulations in SCAPS [30–34].

| Parameter | Value | |
|---|---|---|
| | CdTe | CdS |
| Thickness, μm | 3 | 0.001–0.05 |
| Band gap, eV | 1.5 | 2.4 |
| Electron affinity, eV | 3.9 | 4.0 |
| Dielectric permittivity (relative) | 9.4 | 10.0 |
| CB (conductive band) effective density of states, $cm^{-3}$ | $8.0 \cdot 10^{17}$ | $2.2 \cdot 10^{18}$ |
| VB (valence band) effective density of states, $cm^{-3}$ | $1.8 \cdot 10^{19}$ | $1.8 \cdot 10^{19}$ |
| Electron mobility, $cm^2/(V \cdot sec)$ | $3.2 \cdot 10^2$ | $1.0 \cdot 10^2$ |
| Hole mobility, $cm^2/(V \cdot sec)$ | 40 | 25 |
| Electron thermal velocity (cm/s) | $1.0 \cdot 10^7$ | $1.0 \cdot 10^7$ |
| Hole thermal velocity (cm/s) | $1.0 \cdot 10^7$ | $1.0 \cdot 10^7$ |
| Shallow uniform donor density, $cm^{-3}$ | 0 | $1.1 \cdot 10^{18}$ |
| Shallow uniform acceptor density, $cm^{-3}$ | $2.0 \cdot 10^{14}$ | 0 |

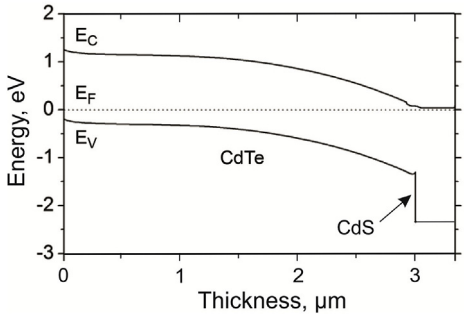


**Fig. 4.** Energy band gap diagram of CdS/CdTe heterojunction under SCAPS modelling.

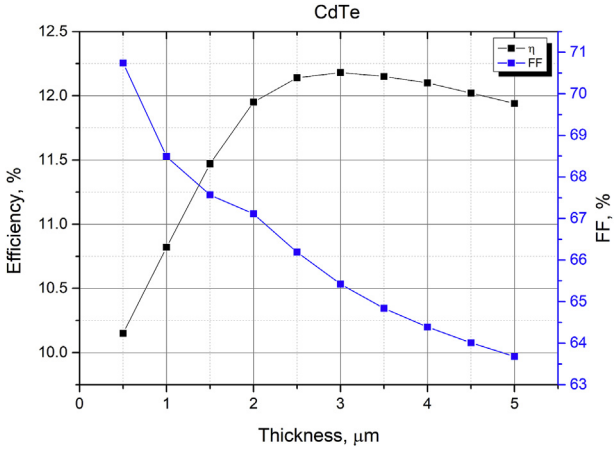


**Fig. 5.** Variation of efficiency η and FF as a function of CdTe absorbing layer thickness.

efficiency of thin films solar cells was 15.77%.

In the present contribution, two set of graphics J-V and Q(λ) are used to characterize CdS/CdTe thin film heterostructure. J-V dependence is the most commonly used tool for characterization of solar cell devices. The measurements were simulated in light under the solar spectrum with an incident solar power of P = 1000 $W/m^2$ at temperature of 300 K. Fig. 7 shows the simulated J-V curves and table shows the values of $V_{oc}$, $J_{sc}$, FF and efficiency at various thickness of CdS window layer with thickness of CdTe absorbing layer d = 3 μm. As can be seen on Fig. 7, the $V_{oc}$ and $J_{sc}$ decrease due to increase the thickness of CdS window layer, and thus, the efficiency is reduced.

Quantum efficiency (QE) is the ratio of the number of charge

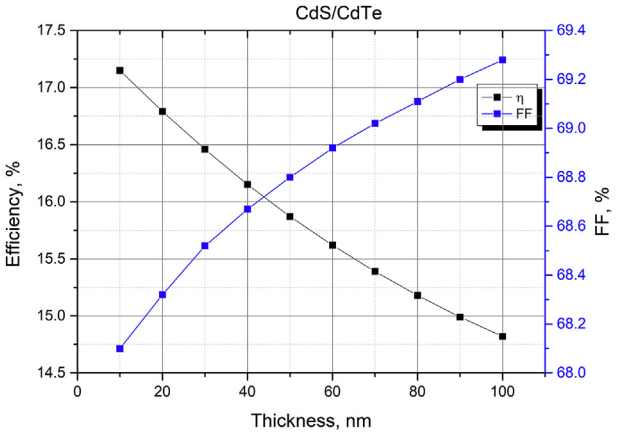


**Fig. 6.** Variation of efficiency η and FF for CdS/CdTe heterojunction as a function of CdS window layer thickness, ($d_{CdTe}$ = 3 μm).

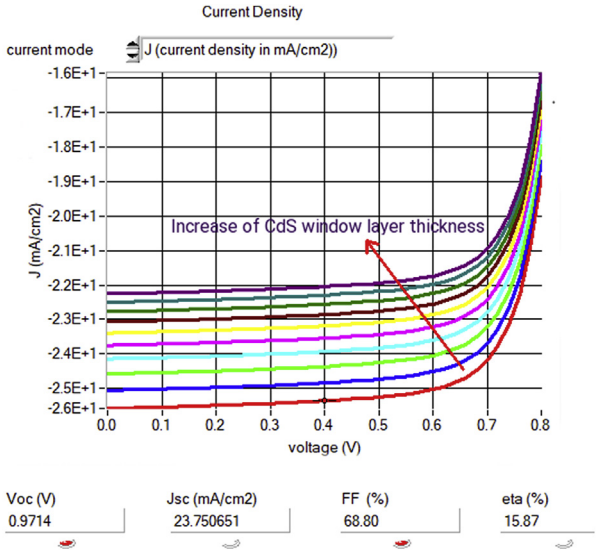


**Fig. 7.** J-V characteristics for CdS/CdTe heterostructure solar cell.

carriers collected by a solar cell to the number of photons of a given energy incident on the solar cell and was calculated according to equation:

$$QE\,[\%] = \frac{number\ of\ reacted\ electrons}{number\ of\ incident\ photons} \times 100\% \quad (3)$$

It is related to the response of a solar cell to the various wavelengths in the spectrum of light which is incident to the cell. The effect of thickness of the absorber layer on quantum efficiency of the cell has been analyzed. Fig. 8 shows the curve of quantum efficiency (QE) as a function of wavelength of the solar cell structure CdS/CdTe with different CdS layer thicknesses. Experimentally, the thickness of CdS window layer varied from 10 nm up to 100 nm, while other input parameters of CdTe absorber layer with thickness d = 3 μm were constant. Fig. 8 shows a part of this range, namely, from 10 nm up to 100 nm. The CdS layer thickness of 50 nm is the technologically minimal limit for the open evaporation method, and this value has the best efficiency for the entire range of thicknesses. Decreasing the thickness of CdS window layer leads directly to increase the performance of CdTe absorber layer solar cells through decreasing the absorption losses that take place in window layer as well as higher short-circuit current might be achieved. Moreover, reducing the thickness of CdS increases the possibility of diffusion of CdS to CdTe during the solar cell fabrication process. Such diffusion between window layer and absorber layer can reduce the strain arising from lattice mismatch and thus causes a reduction of defects in the interface [50]. But it is difficult to obtain uniform and pinhole free CdS layers thinner than 50 nm [51,52].

According to Fig. 8, the cell efficiency increases when the thickness of absorbing layer is decreasing. The decrease of CdS window layer thickness leads to an increase in the quantum efficiency up to 17.15% for 10 nm thickness with a fill factor FF of 68.10%, open circuit voltage $V_{OC}$ of 0.9848 V and a short circuit current density $J_{SC}$ of 25.58 mA/cm$^2$. The highest efficiency was achieved for simulated structure containing CdS window layer (thickness 10 nm) on the CdTe absorber layer (thickness 3 μm). The quantum efficiency is reduced by the surface recombination, reflection and low diffusion length.

As we see from Fig. 8, a decrease in QE for wavelengths below ~530 nm is related to CdS layer thickness. Almost the ideal horizontal line corresponds to a simulated CdS layer thickness of 10 nm. Below there is a line that corresponds to the thickness of 100 nm. However, it is technical limit by using of thermal evaporation method to achieve a certain critical thickness of the emitter layer, below which the film will not be smooth, and only some nanosized formations on the surface of CdTe will be observed. This research indicates that optimal thickness of such CdS formation on CdTe films is about 50 nm. This thickness is theoretically limited under differences in the binding energies of the CdS structure relative to CdTe.

The smaller lattice constant of CdS (compared to CdTe) causes the occurrence of internal tensions (Fig. 9). For the stable and smooth CdS film structure, its internal binding energy value must be higher than the CdS—CdTe interface binding energy. The corresponding amount of internal energy is provided by the critical minimum number of the atomic layers of CdS. It has been experimentally presented that the minimum thickness of CdS is ~50 nm. Considering that the lattice constant of CdS is equal to 0,41365 nm, then such estimated thickness corresponds to ~100–150 atomic layers.

### 3.2. Morphology

The surface homogeneity of the obtained heterostructures was determined additionally by the Nexus 412 Optical Microscope, which makes it possible to determine the presence of phases of various materials in the base material and to investigate the defect structure of the film. The surface images of samples No 21 and No 24 obtained on glass substrates were received with high resolution (camera zoom were 10x, 40x). The scanning was carried out along the X—Y axes, and the measuring range on the samples is 120 × 120 μm (Figs. 10 and 11). These results were processed using specialized software HardworX.

The uniformly distributed grains of CdS (Fig. 10, b) and CdTe (Fig. 11, b) have been observed on the surface of deposited films. This is associated with high evaporation temperature. It can be assumed that these grains are the separate phases of deposited compound. As can be seen from images, received with measuring device, the shape and size of these grains are changeable.

During image processing of heterostructures using Nexus 412 it was observed that with change of lens position above the surface of the sample the sharpness of the image changes. This fact explains irregularity and heterogeneity of the surface of thicker films (Fig. 10, a). For thin films separated phases are not observed (Fig. 11, a). Such surface is more ordered and smooth.

### 3.3. Optical properties

Optical investigation of thin films can provide information about transmittance, thickness, some physical properties (refractive index, absorption coefficient), band gap energy, band structure, and optically active defects [53].

The optical measurements carried out using Agilent Technologies Cary Series UV–Vis–NIR Spectrophotometer in the wavelength range

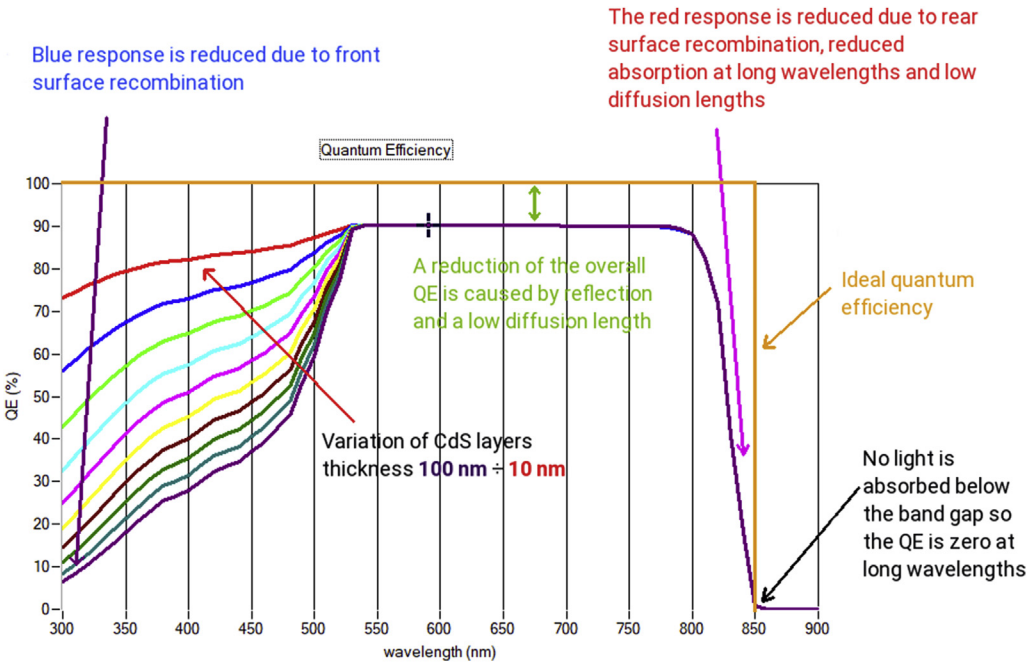


**Fig. 8.** Spectral response of the CdS/CdTe solar cell heterostructure with various thicknesses of CdS window layer.

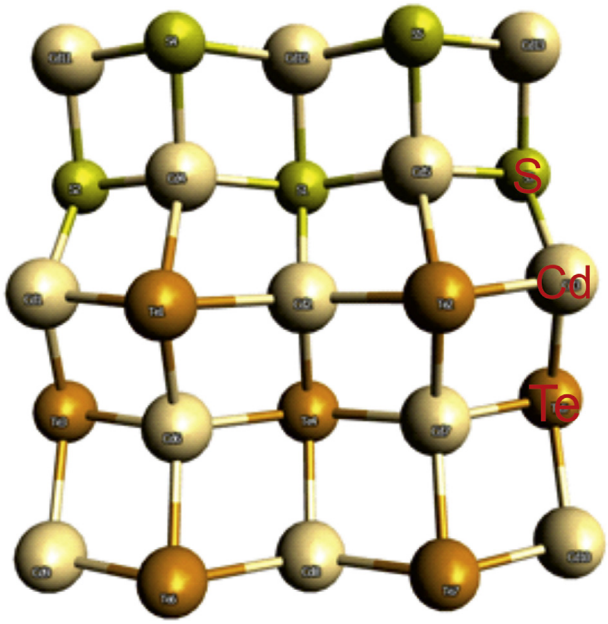


**Fig. 9.** 2D model of CdS layers (two upper layers) on CdTe film (three down layers).

from 180 to 3300 nm. Optical properties of CdTe films have been calculated from transmission T spectra of the films.

The effects of thickness and heterojunction properties on the optical transmittance of CdTe and CdS/CdTe films have been studied. The region of fundamental absorption was observed in transmission spectra. The transmittance curves of CdTe and CdS/CdTe thin films deposited on glass substrates with different thicknesses are shown in Fig. 12. It can be noticed that films are highly transparent in the near-IR region. Absorption edge is about 790–810 nm for all samples, that is completely consistent with the bandgap width of CdTe thin films [54]. The transmittance values that reach up to 90% indicate the high transparency of the as-deposited CdTe thin films (Fig. 12). For a thick film CdTe sample No 21 (Fig. 11, a) a smoother growth of the transmittance with a wavelength increase is observed compared to the film CdTe sample No 24 (Fig. 12, b).

To obtain the optical band gap, the absorption coefficient was derived from the following relation using the transmission data:

$$\alpha = \frac{\ln(1/\tau)}{d} \quad (4)$$

where $d$ is the film thickness and $T$ is the transmittance.

Absorption coefficient versus photon energy is shown in Fig. 13. Using linear approximation these graph dependences allow assessing the value of the energy gap with sharp edge absorption. All samples are characterized by similar width of the optical band gap and it is within a range of 1.46 eV, which is in a good agreement with reference [54]. On the other hand, beyond the band gap edge the absorbance is very small and the transmittance has a high value. This indicates low amount of impurities and lattice defects in the structure of obtained films. In addition, the flat range of the transmission curves without interference fringes emphasizes the surface homogeneity with small crystallite size.

The transmission strongly depends on the film structure, which is determined by the preparation methods, film thickness and deposition modes [55]. The presence of interference patterns in the optical transmission spectra is the indication of the thickness homogeneity of deposited films and smooth surface morphology [56]. It should be noted, that the number of “interference maxima” also depends on the thickness of the film, since at lower film thickness, the interference extremes are spaced further apart and interpolation between these extremes is more difficult. This also could be explained by the fact that there is a difference between the refractive indexes of the film and substrate and due to the interference of multiple light reflections in Fig. 14 [54].

Transmittance values for CdS/CdTe heterojunction are slightly lower than those for pure CdTe films, that may be attributed to greater reflection or scattering effects in film thickness, structural heterogeneity and worse crystallinity [57]. The absorption process of the films is complex and may occur due to light scattering in transparent regions, defect absorption, multi-phonon absorption, or Urbach tail [58,59].

One of the most popular analysis methods applied to transmission spectrum to determine the optical properties of the material is the Swanepoel method [26]. Nowadays this method found its way into

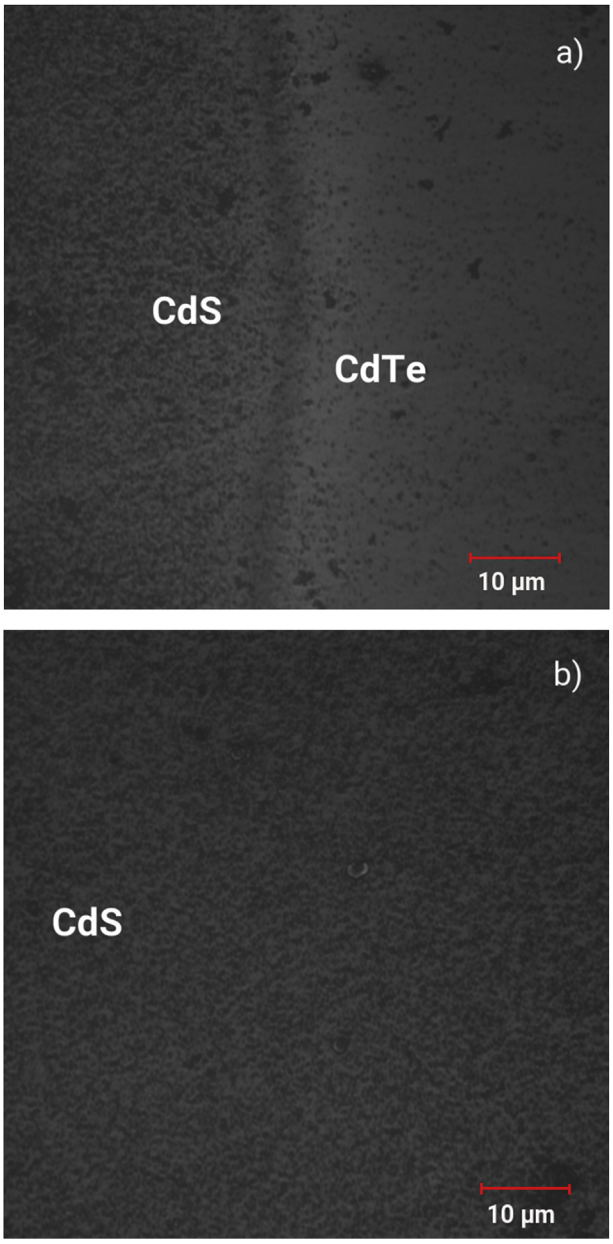


**Fig. 10.** Surface image: a) CdS/CdTe heterojunction; b) CdS thin film (sample No 21, 40x camera zoom).

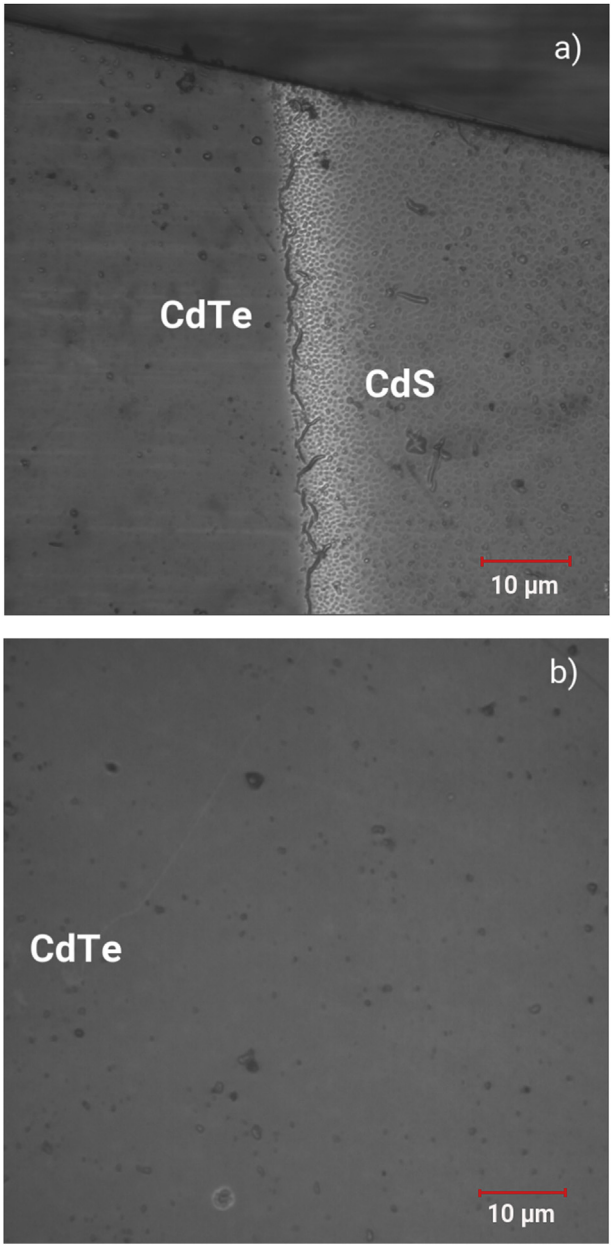


**Fig. 11.** Surface image: a) CdS/CdTe heterojunction; b) CdTe thin film (sample No 24, 40x camera zoom).

commercial thin film manufacturing [60,61]. Swanepoel method is applicable to any transmission spectrum showing appreciable interference fringes, when well resolved interference extrema are visible. The envelope method is highly useful and very straightforward. It gives the same results as the other analysis methods, but evidently only yields refractive index values at the wavelengths corresponding to the extremes of the interference fringes.

The mechanism of transmission and reflection in the film thickness on a transparent substrate looks like it is shown in Fig. 14, where $n$, $\alpha$, $d$ and $T$ denote the refractive index, absorption coefficient, thickness and transmittance of the film, respectively.

The transparent substrate has a thickness of several orders of magnitude larger than index of refraction $n_0 = 1$, absorption coefficient $\alpha_s = 0$ and transmittance $T_s$ for the system consisting of a thin film on transparent substrate surrounded by air and taking into account all multiple reflections at the interface. If the thickness $d$ is uniform then the interference effects generate a spectrum. As it was mentioned above, the interference fringes were used to calculate the optical constants of the film such as refractive index, film thickness and absorption coefficient.

The transmittance $T$ for the normal incidence resulted from the interference of the wave transmitted from three interfaces can be calculated by relation (5). The calculated values of $d$ and $x$ are used as initial least-square fitting parameters for the following equation [26]:

$$T = T(n, x) = \frac{Ax}{B - Cx\cos(\varphi) + Dx^2} \tag{5}$$

where

$$A = 16n^2 s \tag{6}$$

$$B = (n + 1)^3(n + s^2) \tag{7}$$

$$C = 2(n^2 - 1)(n^2 - s^2) \tag{8}$$

$$D = (n - 1)^3(n - s^2) \tag{9}$$

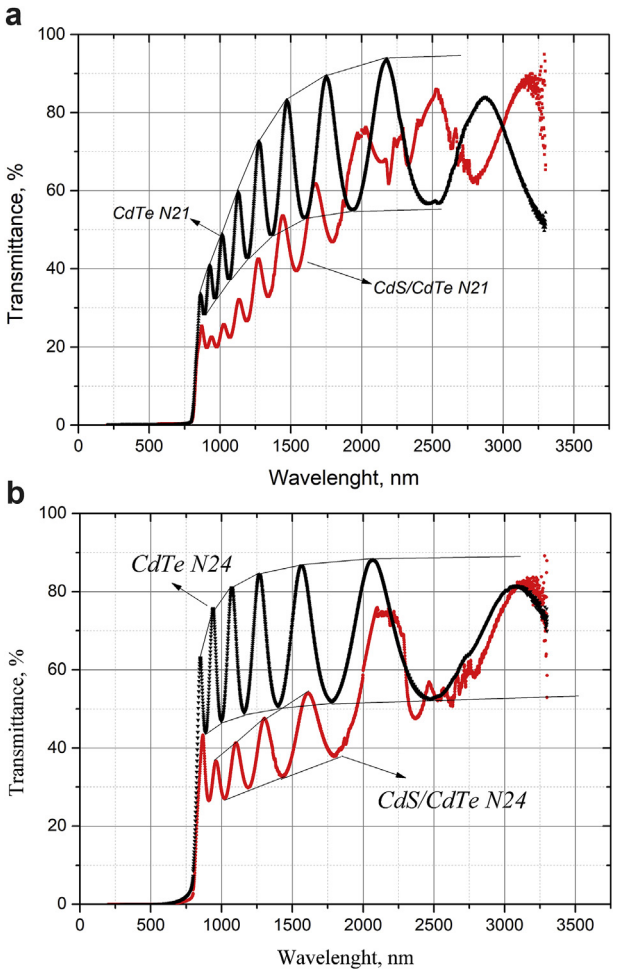


**Fig. 12.** Optical transmission spectra for: *a)* CdTe (sample No 21); CdS/CdTe (sample No 21); *b)* CdTe (sample No 24); CdS/CdTe (sample No 24).

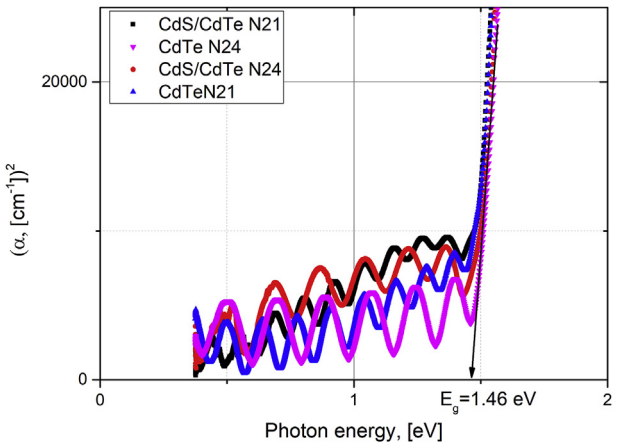


**Fig. 13.** Absorption spectra in Tauc coordinates of CdTe thin film and CdS/CdTe heterojunctions.

$$\varphi = \frac{4\pi nd}{\lambda} \tag{10}$$

$$x = e^{-\alpha d} \tag{11}$$

Maximum and minimum of interference fringes are determined from the following equations:

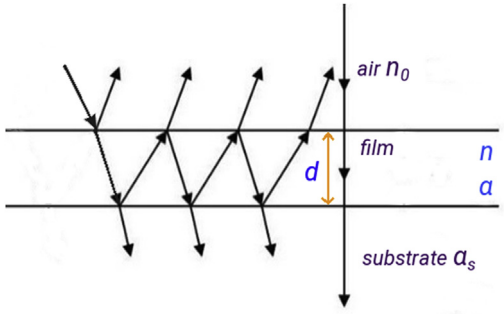


**Fig. 14.** Schematic diagram of a thin film on the substrate. Arrows indicate transmission and reflection at different interfaces.

$$T_M = \frac{Ax}{B - Cx + Dx^2} \tag{12}$$

$$T_m = \frac{Ax}{B + Cx + Dx^2} \tag{13}$$

The refractive index of the substrate is found from the following relation, where $T_s$ is the maximum value of the transmittance of substrate:

$$s = \frac{1}{T_s} + \left(\frac{1}{T_s^2} - 1\right)^{\frac{1}{2}} \tag{14}$$

From the above equations, the refractive index $n$ is established:

$$n = \left(N + (N^2 - s^2)^{\frac{1}{2}}\right)^{\frac{1}{2}} \tag{15}$$

where

$$N = \frac{2s(T_M - T_m)}{T_M T_m} + \frac{s^2 + 1}{2} \tag{16}$$

Applying equation (15) – (16) and taking into account that refractive index of the substrate s = 0.92, the refractive indexes of samples CdTe and CdS/CdTe can be calculated. The ranges of frequencies in which films weakly absorb denote the refractive index. Fig. 15 shows the variation of refractive index of CdTe films and the average values are about 2.48 for a sample No 21 and 2.45 for a sample No 24. These values are completely consistent with the literary ones that matter for CdTe thin films to 2.5 [62]. For CdS/CdTe heterojunction these values are about 2.52 for sample No 21 and 2.72 for sample No 24. These values are consistent with [63].

The thickness (d) of the film can be determined by the following equation:

$$d = \frac{\lambda_1 \lambda_2}{2(\lambda_1 n_2 - \lambda_2 n_1)} \tag{17}$$

where $n_1$ and $n_2$ are the refractive indices of the $\lambda_1$ and $\lambda_2$ wavelength calculated for two adjacent maxima or minima. The average value of the theoretical thickness $^{<}d^{>}$ of CdS/CdTe heterostructure calculated by Swanepoel's method is 1657.58 nm for the sample No 21 (experimental value is 1685 nm) and for the sample No 24 it equals 1441.13 nm (experimental value – 1485 nm). The measured values of the thickness were received using the profilometer method (Table 1).

Therefore, comparing the experimental and calculated data for the thickness values, the presence of a small difference in values can be noted, that may be associated with error in the data calculating processes.

The order of interference m at the maxima of transmission spectra is determined as:

$$m = \left(\frac{\lambda_2}{\lambda_1 - \lambda_2}\right) \tag{18}$$

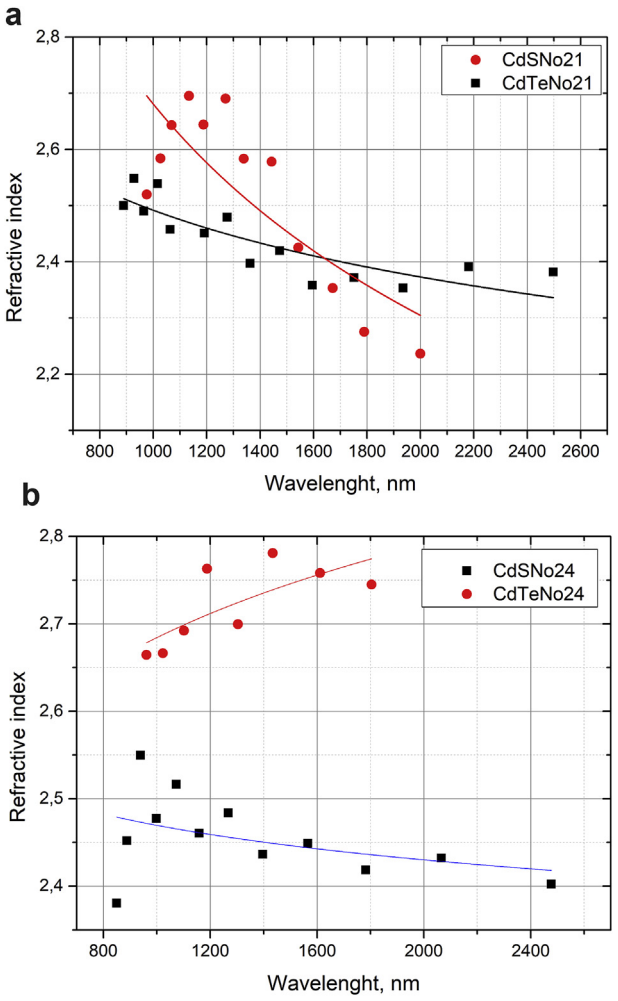


**Fig. 15.** Refractive index versus wavelength for: *a)* CdTe (sample No 21), CdS/CdTe (sample No 21); *b)* CdTe (sample No24); CdS/CdTe (sample No24).

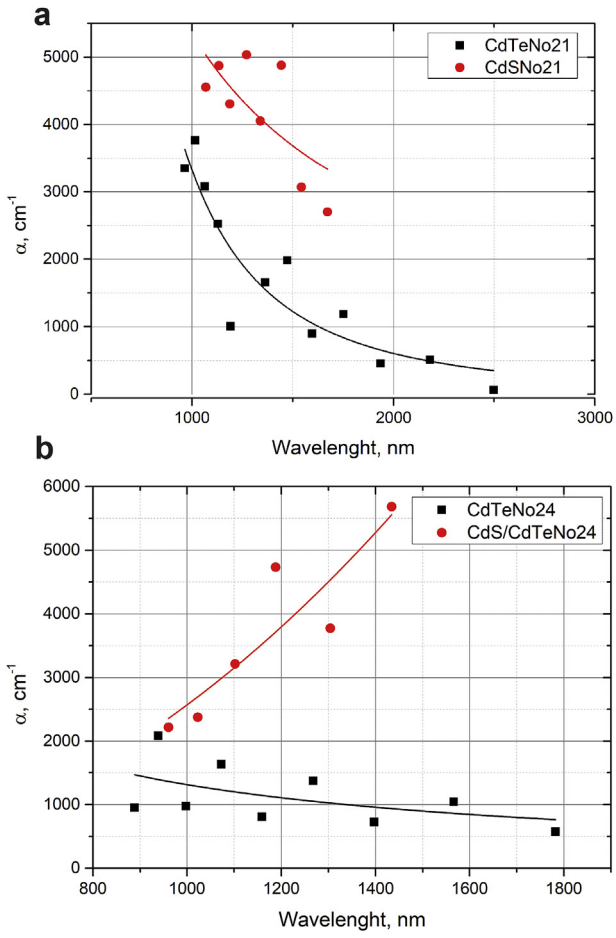


**Fig. 16.** Absorption coefficient versus wavelength for: *a)* CdTe (sample No 21), CdS/CdTe (sample No21); *b)* CdTe (sample No 24), CdS/CdTe (sample No24).

where $\lambda_1$ and $\lambda_2$ are the wavelengths of two adjacent transmission maxima ($\lambda_1 > \lambda_2$).

For a region where presence of a strong light absorption is observed, the absorption coefficient is determined as follows:

$$\alpha = \frac{1}{d} ln \frac{(n-1)^3(n-s^2)}{Em - (E_m^2 - (n^2-1)^3(n^2-s^4))^{0.5}} \quad (19)$$

where

$$E_m = \left(\frac{8n^2 s}{T_m}\right) - (n^2-1)(n^2-s^2) \quad (20)$$

For CdS/CdTe heterojunction a significant increase the light absorption in several times, primarily in the short-wave region of the spectrum (Fig. 16) takes place. This is due to the fact that CdS thin layer through the large band gap (2.42 eV) plays the role of «absorbing window».

The photons absorbed in the window layer do not contribute to the photocurrent, as recombination is very likely to occur, resulting in scattering of light. Therefore, absorption in the CdS layer is a source for significant losses.

For samples No 21 and No 24, a visible difference in absorption coefficients in graphs is presented. It can be noted that the absorption coefficient for thin films of CdTe acquires larger values than for the CdS/CdTe heterojunctions at the corresponding wavelengths for both specimens.

## 4. Conclusions

CdTe thin films and CdS/CdTe heterojunction were deposited on glass substrates with different technological parameters using PVD technique by thermal evaporation method. Analysis of the optical properties of CdTe thin films was performed and their comparing after the addition of an “absorption window” of CdS has been investigated. Optical transmission spectra of thin films were examined with use of Swanepoel method. It was found that the thin layer of CdS causes significantly increase in the absorption properties of the films. The thickness of the film is theoretically calculated and the obtained results coincide with the experimental studies by profilometer. The optimal thickness of the CdS layer for the best values of the efficiency of the CdS/CdTe heterojunction 15.8% was optimized in the SCAPS software for simulation of the optical parameters. Comparing the analysis of quantum efficiency QE and technological modes allowed obtaining optimal properties for the CdS layer about 50 nm. It is shown that CdS/CdTe heterojunctions have good prospects of using as photovoltaic light converters due to their high absorption capacitance. The conditions of obtaining of CdTe thin films and CdS/CdTe heterojunction on glass substrates by thermal evaporation method allowed getting qualitative transmission spectra.

## Declaration of interest

None.

## References


[1] M.A. Green, K. Emery, Y. Hishikawa, W. Warta, Solar cell efficiency tables (version 37), Prog. Photovoltaics Res. Appl. 19 (1) (2011) 84–92 https://doi.org/10.1002/pip.1088.

[2] R. Swami, Solar cell, Int. J. of Sci. Res. Publ. 2 (7) (2012) 1–5 2250–3153.

[3] G. Hiscock, Earth Wars: the Battle for Global Resources, John Wiley & Sons, Singapore, 2012.

[4] S.G. Kumar, K.K. Rao, Physics and chemistry of CdTe/CdS thin film heterojunction photovoltaic devices: fundamental and critical aspects, Energy Environ. Sci. 7 (1) (2014) 45–102 https://doi.org/10.1039/C3EE41981A.

[5] H. Movla, Optimization of the CIGS based thin film solar cells: numerical simulation and analysis, Opt.-Intern. J. Light Electr. Opt. 125 (1) (2014) 67–70 https://doi.org/10.1016/j.ijleo.2013.06.034.

[6] H. Kim, K. Cha, V.M. Fthenakis, P. Sinha, T. Hur, Life cycle assessment of cadmium telluride photovoltaic (CdTe PV) systems, Sol. Energy 103 (2014) 78–88 https://doi.org/10.1016/j.solener.2014.02.008.

[7] L. Kosyachenko, T. Toyama, Current–voltage characteristics and quantum efficiency spectra of efficient thin-film CdS/CdTe solar cells, Sol. Energy Mater. Sol. Cells 120 (2014) 512–520 https://doi.org/10.1016/j.solmat.2013.09.032.

[8] L. Zhi, F. Lianghuan, Z. Guanggen, L. Wei, Z. Jingquan, W. Lili, W. Wenwu, Influence of CuxS back contact on CdTe thin film solar cells, J. Semicond. 34 (1) (2013) 014008https://doi.org/10.1088/1674-4926/34/1/014008.

[9] D. Bonnet, H. Rabenhorst, New results on the development of a thin-film p-CdTe-n-CdS heterojunction solar cell, Photovoltaic Specialists Conference, 9 th, Silver Spring, Md, 1972.

[10] K.W. Mitchell, A.L. Fahrenbruch, R.H. Bube, Evaluation of the CdS/CdTe heterojunction solar cell, J. Appl. Phys. 48 (10) (1977) 4365–4371.

[11] Tyan Yuan-Sheng, Polycrystalline thin film CdS/CdTe photovoltaic cell, U.S. Patent No. 4,207,119. 10 Jun; 1980.

[12] X. Wu, J.C. Keane, R.G. Dhere, C. DeHart, A. Duda, T.A. Gessert, S. Asher, D.H. Levi, P. Sheldon, 16.5%-efficient CdS/CdTe polycrystalline thin-film solar cell, Proceedings of the 17th European Photovoltaic Solar Energy Conference, vol 995, James & James Ltd., London, 2001.

[13] X. Wu, High-efficiency polycrystalline CdTe thin-film solar cells, Sol. Energy 77 (6) (2004) 803–814.

[14] Morales-Acevedo Arturo, Thin film CdS/CdTe solar cells: research perspectives, Sol. Energy 80 (6) (2006) 675–681.

[15] First solar sets world record for CdTe solar PV efficiency. First solar, http://investor.firstsolar.com/releasedetail.cfm?ReleaseID = 593994 , Accessed date: 6 January 2015.

[16] First Solar sets 18.7% record for CdTe solar cell efficiency. Semiconductor today, http://www.semiconductor-today.com/news_items/2013/FEB/FIRSTSOLAR_260213.html , Accessed date: 6 January 2015.

[17] First solar sets new world record for CdTe solar cell efficiency. First solar, http://investor.firstsolar.com/releasedetail.cfm?Releaseid = 743398 , Accessed date: 6 January 2015.

[18] First Solar acquires GE thin film technology unit. PV magazine, http://www.pvmagazine.com/news/details/beitrag/first-solar-acquires-ge-thin-film-technologyunit_100012279/#axzz3idk970gD , Accessed date: 6 February 2015.

[19] First Solar sets world record for CdTe solar cell efficiency. First solar, http://investor.firstsolar.com/releasedetail.cfm?ReleaseID = 828273 , Accessed date: 6 February 2015.

[20] First Solar builds the highest efficiency thin film PV cell on record. First solar, http://investor.firstsolar.com/releasedetail.cfm?ReleaseID = 864426 , Accessed date: 6 February 2015.

[21] http://investor.firstsolar.com/releasedetail.cfm?ReleaseID = 956479.

[22] T.D. Lee, A.U. Ebong, A review of thin film solar cell technologies and challenges, Renew. Sustain. Energy Rev. 70 (2017) 1286–1297 https://doi.org/10.1016/j.rser.2016.12.028.

[23] R.S. Yavorskyi, Z.R. Zapukhlyak, Y.S. Yavorskyi, L.I. Nykyruy, Vapor phase condensation for photovoltaic CdTe films, Phys. and Chem. Solid State 18 (4) (2017) 410–416 https://doi.org/10.15330/pcss.18.4.416.

[24] M.J. Kim, H.T. Kim, J.K. Kang, D.H. Kim, D.H. Lee, S.H. Lee, S.H. Sohn, Effects of the surface roughness on optical properties of CdS thin films, Mol. Cryst. Liq. Cryst. 532 (1) (2010) 21/[437]–28/[444] https://doi.org/10.1080/15421406.2010.497099.

[25] J.C. Manifacier, J. Gasiot, J.P. Fillard, A simple method for the determination of the optical constants n, k and the thickness of a weakly absorbing thin film, J. Phys. E Sci. Instrum. 9 (11) (1976) 1002 https://doi.org/10.1088/0022-3735/9/11/032.

[26] R. Swanepoel, Determination of the thickness and optical constants of amorphous silicon, J. Phys. E Sci. Instrum. 16 (12) (1983) 1214 https://doi.org/10.1088/0022-3735/16/12/023.

[27] R. Swanepoel, Determination of surface roughness and optical constants of inhomogeneous amorphous silicon films, J. Phys. E Sci. Instrum. 17 (10) (1984) 896 https://doi.org/10.1088/0022-3735/17/10/023.

[28] F.J. Alvarez, N. Di Lalla, A. Lamagna, Thin film CdS/CdTe solar cells prepared by electrodeposition using low cost materials, Conf. Rec. of the Twenty-Sixth IEEE Photovolt. Spec. Conf. 1997, pp. 459–462 https://doi.org/10.1109/PVSC.1997.654127.

[29] L.A. Kosyachenko, A.I. Savchuk, E.V. Grushko, Dependence of efficiency of thin-film CdS/CdTe solar cell on parameters of absorber layer and barrier structure, Thin Solid Films 517 (7) (2009) 2386–2391 https://doi.org/10.1016/j.tsf.2008.11.012.

[30] H.A. Mohamed, Influence of the optical and recombination losses on the efficiency of CdS/CdTe solar cell at ultrathin absorber layer, Can. J. Phys. 92 (11) (2014) 1350–1355 https://doi.org/10.1139/cjp-2013-0477.

[31] L.A. Kosyachenko, E.V. Grushko, V.V. Motushchuk, Recombination losses in thin-film CdS/CdTe photovoltaic devices, Sol. Energy Mater. Sol. Cells 90 (15) (2006) 2201 https://doi.org/10.1016/j.solmat.2006.02.027.

[32] V.V. Brus, On quantum efficiency of nonideal solar cells, Sol. Energy 86 (2) (2012) 786–791 https://doi.org/10.1016/j.solener.2011.12.009.

[33] H.A. Mohamed, Dependence of efficiency of thin-film CdS/CdTe solar cell on optical and recombination losses, J. Appl. Phys. 113 (9) (2013) 093105https://doi.org/10.1063/1.4794201.

[34] A. Morales-Acevedo, N. Hernández-Como, G. Casados-Cruz, Modeling solar cells: a method for improving their efficiency, Mater. Sci. Eng. B177 (16) (2012) 1430–1435 https://doi.org/10.1016/j.mseb.2012.01.010.

[35] A. Aissat, R. Bestam, J.P. Vilcot, Modeling and simulation of $Al_xGa_yIn_{1-x-y}As/InP$ quaternary structure for photovoltaic, Int. J. Hydrogen Energy 39 (27) (2014) 15287–15291 https://doi.org/10.1016/j.ijhydene.2014.04.162.

[36] D. Wang, H. Cui, G. Su, A modeling method to enhance the conversion efficiency by optimizing light trapping structure in thin-film solar cells, Sol. Energy 120 (2015) 505–513 https://doi.org/10.1016/j.solener.2015.07.051.

[37] H. Arbouz, A. Aissat, J.P. Vilcot, Modeling and optimization of $CdS/CuIn_{1-x}Ga_xSe_2$ structure for solar cells applications, Internat. J. Hydrog. Energy 41 (45) (2016) 20987–20992 https://doi.org/10.1016/j.ijhydene.2016.06.104.

[38] L. Nykyrui, Y. Saliy, R. Yavorskyi, Y. Yavorskyi, V. Schenderovsky, G. Wisz, S. Górny, CdTe vapor phase condensates on (100) Si and glass for solar cells, 7th Internat. Conf. On Nanomater. – Appl. & Prop. (NAP), 2017 01PCSI26-1 https://doi.org/10.1109/NAP.2017.8190161.

[39] M. Burgelman, J. Verschraegen, S. Degrave, P. Nollet, Modeling thin-film PV devices, Prog. Photovoltaics Res. Appl. 12 (2-3) (2004) 143–153 https://doi.org/10.1002/pip.524.

[40] M. Burgelman, P. Nollet, S. Degrave, Modelling polycrystalline semiconductor solar cells, Thin Solid Films 361 (2000) 527–532 https://doi.org/10.1016/S0040-6090(99)00825-1.

[41] M. Burgelman, J. Marlein, Analysis of graded band gap solar cells with SCAPS, Proc. Of the 23rd Eur. Photovolt. Sol. Energy Conf., Valencia, 2008, pp. 2151–2155 https://doi.org/1854/LU-678258.

[42] J. Verschraegen, M. Burgelman, Numerical modeling of intra-band tunneling for heterojunction solar cells in SCAPS, Thin Solid Films 515 (15) (2007) 6276–6279 https://doi.org/10.1016/j.tsf.2006.12.049.

[43] S. Degrave, M. Burgelman, P. Nollet, Modelling of polycrystalline thin film solar cells: new features in scaps version 2.3, Proc. Of 3rd World Conf. on Photovolt. Energy Convers, vol 1, 2003, pp. 487–490.

[44] M. Gloeckler, A.L. Fahrenbruch, J.R. Sites, Numerical modeling of CIGS and CdTe solar cells: setting the baseline, Proc. Of 3rd World Conf. on Photovolt. Energy Convers, vol 1, 2003, pp. 491–494.

[45] H. Zerfaoui, D. Dib, M. Rahmani, K. Benyelloul, C. Mebarkia, Study by simulation of the $SnO_2$ and ZnO anti-reflection layers in n-SiC/p-SiC solar cells, AIP Conf. Proc. 1758 (1) (2016) 030029https://doi.org/10.1063/1.4959425.

[46] C. Dumitrache, N. Olariu, E. St Lakatos, G. Mantescu, L. Olteanu, M. Badea, Some new features of SCAPS 2902 used for optimisation of CdS-CdTe thin-film photovoltaic cell structure, Electrotehnica Electr. Automat. 61 (1) (2013) 25.

[47] S. Khosroabadi, S.H. Keshmiri, Design of a high efficiency ultrathin CdS/CdTe solar cell using back surface field and backside distributed Bragg reflector, Optic Express 22 (103) (2014) A921–A929 https://doi.org/10.1364/OE.22.00A921.

[48] N. Amin, K. Sopian, M. Konagai, Numerical modeling of CdS/CdTe and CdS/CdTe/ZnTe solar cells as a function of CdTe thickness, Sol. Energy Mater. Sol. Cells 91 (13) (2007) 1202–1208 https://doi.org/10.1016/j.solmat.2007.04.006.

[49] G. Calogero, I. Citro, C. Crupi, G. Carini Jr., D. Arigò, G. Spinella, A. Bartolotta, G. Di Marco, Absorption spectra, thermal analysis, photoelectrochemical characterization and stability test of vegetable-based dye-sensitized solar cells, Opt. Mater. 88 (2019) 24–29 https://doi.org/10.1016/j.optmat.2018.11.005.

[50] W. Jaegermann, A. Klein, J. Fritsche, D. Kraft, B. Späth, Interfaces in CdTe solar cells: from idealized concepts to technology, MRS Online Proceedings Library Archive, 2005, p. 865 https://doi.org/10.1557/PROC-865-F6.1.

[51] H. Mohamed, Theoretical study of the efficiency of CdS/PbS thin film solar cells, Sol. Energy 108 (2014) 360–369 https://doi.org/10.1016/j.solener.2014.07.017.

[52] H. Mohamed, A. Mohamed, H. Ali, Theoretical study of ZnS/CdS bi-layer for thin-film CdTe solar cell, Mater. Res. Express 5 (5) (2018) 056411.

[53] G. Wisz, I. Virt, P. Sagan, P. Potera, R. Yavorskyi, Structural, optical and electrical properties of zinc oxide layers produced by pulsed laser deposition method, Nanoscale Res. Lett. 12 (1) (2017) 253 https://doi.org/10.1186/s11671-017-2033-9.

[54] K. Punitha, R. Sivakumar, C. Sanjeeviraja, V. Sathe, V. Ganesan, Physical properties of electron beam evaporated CdTe and CdTe: Cu thin films, J. Appl. Phys. 116 (21) (2014) 213502 https://doi.org/10.1063/1.4903320.

[55] C. Santiago Tepantlán, A.M. Pérez González, I. Valeriano Arreola, Structural, optical and electrical properties of CdS thin films obtained by spray pyrolysis, Rev. Mexic. Fisica 54 (2) (2008) 112–117 0035–001X.

[56] R. Yavorskyi, L. Nykyruy, G. Wisz, P. Potera, S. Adamiak, S. Górny, Structural and optical properties of cadmium telluride obtained by physical vapor deposition technique, Appl. Nanosci. (2018) 1–10 https://doi.org/10.1007/s13204-018-0872-z.

[57] M.H. Jacobs, D.W. Pashley, M.J. Stowell, The formation of imperfections in epitaxial gold films, Philos. Mag. A 13 (121) (1966) 129–156 https://doi.org/10.1080/14786436608211992.

[58] W. Mahmood, J. Ali, A. Thomas, S. ullah Awan, M. Jackman, A.U. Haq, M.U. Hassand, N.A. Shah, Role of $Ag^{1+}$ substitutional defects on the electronic and optical properties of n-type CdS thin films semiconductor for sustainable and stable

window layer in solar cells technology, Opt. Mater. 85 (2018) 143–152 https://doi.org/10.1016/j.optmat.2018.08.056.
[59] W. Mahmood, J. Ali, I. Zahid, A. Thomas, A. ul Haq, Optical and electrical studies of CdS thin films with thickness variation, Optik 158 (2018) 1558–1566 https://doi.org/10.1016/j.ijleo.2018.01.045.
[60] Essential MacLeod, Thin Film, Center Inc., Tucson, AZ, USA, 2018http://www.thinfilmcenter.com , Accessed date: 19 November 2018.
[61] FilmStar, FTG Software Associates, Princeton, NJ, USA, 2018http://www.ftgsoftware.com/design.htm , Accessed date: 19 November 2018.
[62] R.E. Treharne, A. Seymour-Pierce, K. Durose, K. Hutchings, S. Roncallo, D. Lane, Optical design and fabrication of fully sputtered CdTe/CdS solar cells, J. Phys. Conf. Ser. 286 (1) (2011) 012038https://doi.org/10.1088/1742-6596/286/1/012038.
[63] F. Lisco, P.M. Kaminski, A. Abbas, J.W. Bowers, G. Claudio, M. Losurdo, J.M. Walls, High rate deposition of thin film cadmium sulphide by pulsed direct current magnetron sputtering, Thin Solid Films 574 (2015) 43–51 https://doi.org/10.1016/j.tsf.2014.11.065.